PHILOSOPHICAL TRANSACTIONS B

rstb.royalsocietypublishing.org

Chirality of the cytoskeleton in the origins of cellular asymmetry

Peter Satir

Department of Anatomy and Structural Biology, Albert Einstein College of Medicine, Bronx, NY 10461, USA

PS, 0000-0003-3665-9387

Opinion piece

Cite this article: Satir P. 2016 Chirality of the cytoskeleton in the origins of cellular asymmetry. *Phil. Trans. R. Soc. B* **371**: 20150408.
http://dx.doi.org/10.1098/rstb.2015.0408

Accepted: 15 April 2016

One contribution of 17 to a theme issue 'Provocative questions in left–right asymmetry'.

Subject Areas:
cellular biology

Keywords:
bacterial flagellum, actin filament, microtubules, basal body, cilia, asymmetry

Author for correspondence:
Peter Satir
e-mail: satir@aecom.yu.edu

Self-assembly of two important components of the cytoskeleton of eukaryotic cells, actin microfilaments and microtubules (MTs) results in polar filaments of one chirality. As is true for bacterial flagella, in actin microfilaments, screw direction is important for assembly processes and motility. For MTs, polar orientation within the cell is paramount. The alignment of these elements in the cell cytoplasm gives rise to emergent properties, including the potential for cell differentiation and specialization. Complex MTs with a characteristic chirality are found in basal bodies and centrioles; this chirality is preserved in cilia. In motile cilia, it is reflected in the direction of the effective stroke. The positioning of the basal body or cilia on the cell surface depends on polarity proteins. In evolution, survival depends on global polarity information relayed to the cell in part by orientation of the MT and actin filament cytoskeletons and the chirality of the basal body to determine left and right coordinates within a defined anterior–posterior cell and tissue axis.

This article is part of the themed issue 'Provocative questions in left–right asymmetry'.

1. What is the basis of chirality in cells?

The question is whether there is a fundamental molecular basis of organelle chirality that manifests itself in cellular and organ asymmetry; or is cellular asymmetry a property that emerges through self-assembly? Clearly, fundamental molecular chiralities exist: the amino acids of cellular proteins are all of one enantiomorph, L rather than D; α helices in proteins spiral to the right, rarely to the left and so on. In the deepest sense, these molecular chiralities must of course be reflected in cell organization and function, but it is hard, outside the scope of this article and perhaps unproductive to demonstrate that cellular axes or cytoskeletal constructions map directly onto these universal molecular asymmetries.

2. Chirality in cytoskeletal and extracellular filaments

However, because helices are intrinsically chiral, where molecular assembly results in a helix of one specific chirality, some extracellular and cytoskeletal structures, such as bacterial flagella, collagen fibres, actin microfilaments and microtubules (MTs) are intrinsically chiral. Molecular assembly results in a given chirality and all of such helices in or on a cell are of one type. In these cases, the specific helical twist can have important effects on cellular function.

(a) The bacterial flagellum

The bacterial flagellum provides a classical example. The flagellum of *E. coli* or *Salmonella* consists of an extracellular helical filament comprised of the protein flagellin attached by a hook to a rotary motor consisting of a series of intramembrane and peripheral membrane proteins. The motor produces either clockwise or anticlockwise high-speed rotation using ion motive force [1]. When the motor drives the filament anticlockwise (viewed looking downwards from the filament towards the cell), several neighbouring filaments with left-handed helices become coupled hydrodynamically into a bundle that screws

THE ROYAL SOCIETY PUBLISHING

through the medium producing a more or less straight line motion known as a run. However, randomly (with a frequency that can be biased by chemotaxis) the motor can switch to clockwise rotation. This causes the filament to transform from a left-handed to a right-handed helix, which in turn causes the filament bundle to fly apart with each filament producing directionally uncoordinated motion, causing the cell to tumble. When anticlockwise rotation resumes, the bundle reforms to propel the cell in a new direction. The different helical forms are produced by supercoiling of the flagellin protofilaments in different conformations and packings [2]. In this case, chiral helical structure clearly has implications for function.

(b) Actin microfilaments

(i) Filament rotation

Actin microfilaments are helices and here too, chirality is critical to movement. Nishizaka *et al*. [3] used an *in vitro* system of heavy meromyosin and an actin filament to demonstrate that a right-handed rotation of the supercoiled helical filament is essential to sliding and presumably to muscle contraction [4].

It is possible to construct a rotary motor *in vitro* using isolated F1-ATPase found in mitochondrial or bacterial membranes. A helical actin filament may be attached to the motor and it will rotate when ATP is added as an energy source [5]. This system is analogous to the bacterial flagellum, although the rotation is much slower. Viscoelastic properties of the rotating actin filament have been determined, although no one seems to have used this system to examine changes in helical structure during rotation.

(ii) The Limulus acrosome

Actin microfilaments may be tightly packed into bundles where all the helices are aligned. One well-studied excellent example is the Limulus acrosomal process where helices are cross-linked by the protein scruin and stimulation produces an explosive extension of the bundle from the sperm head to penetrate the egg [6]. Changing the helical twist provides energy for motion and the force for fertilization [7].

(iii) Listeria propulsion and motility by actin polymerization

As first described by Tilney & Portney [8], Listeria, an intracellular bacterial pathogen, propels itself through host cell cytoplasm by polymerization of an actin comet tail. Basically, actin polymerizes at the rear end of the bacterium above a transmembrane protein Act A using an elastic Brownian rachet mechanism [9] where G-actin monomers are inserted at the end of a growing helical filament. Eventually, the tail with multiple cross-linked actin filaments forms. The elastic properties of this bundle that give rise to motility have been extensively modelled [10]. Using Act-A–coated polystyrene beads, Cameron *et al*. [11] (and others) provides an example to show that polymerization and movement can be reproduced *in vitro*. Brownian rachet mechanisms may be generally important in actin polymerization events such as lamellipod formation in cell motility.

(iv) Microvilli and stereocilia

In microvilli such as those of the brush border of mammalian intestine, individual actin filaments are aligned in a superstructure with all helices oriented in the same direction uniformly giving rise to barbed ends at the tip of the microvillus and pointed ends in the cell cortex. Such structural uniformity can be easily demonstrated by binding heavy meromyosin to the filaments. The actin filaments are attached to the microvillar membrane by a spiralling array of myosin-1a motor molecules [12]. When ATP is hydrolysed, the myosin walks along the actin filaments producing a tip-end directed translation of the membrane which is then shed into the intestinal lumen from the tip as small vesicles [13]. Reciprocally, the actin bundle screws down into the cortex.

Stereocilia are a misnomer because they are not cilia but modified microvilli best characterized on hair cells of the vertebrate ear. Like microvilli, they are composed of uniformly oriented cross-linked actin filaments, but unlike brush border microvilli the length of filament bundle varies systematically along the cell. The actin bundles can be very slightly bent by fluid motion or mechanical stimuli [14]. Bending pushes the actin filaments toward the cell cortex and stretches an extracellular link coupling the tips of adjacent stereocilia to initiate the opening of transmembrane channels.

(v) Striated muscle

Helical actin filaments of the I band screw into the thick myosin-2 filaments to produce sarcomere shortening. However, an important new distinction for discussion of chirality in cells, tissues and organisms is seen here. While all the actin filaments on one side of the Z line are aligned as is the case for microvilli, and while the helical nature of the filaments is the same on both sides of the Z line, the polarity of direction of screw reverses at the Z line—thus producing a left and right side of oppositely oriented actin bundles [15]. The intrinsic polar nature of the filaments does not change, yet the cell has a new chiral property: for example, if only one side of the I band, say to the left of the Z line, is activated, the cell will move left [16,17].

(c) Microtubules

MTs are comprised of $\alpha\beta$ tubulin heterodimers polymerized head to tail into micrometre long protofilaments arranged in an approximately 25 nm ring. In the MT, each protofilament has the same polarity giving the MT a fast-polymerizing β tubulin (+) and a slow-polymerizing α tubulin (−) end. When polymerized from purified tubulin *in vitro*, the number of protofilaments in the microtubule wall can vary from roughly 10–17. *In vivo* MTs are predominantly comprised of 13 protofilaments, which run parallel to the MT axis. MTs with different protofilament numbers are each constructed slightly differently [18]. This may have interesting consequences. In *Arabidopsis*, mutant tubulins probably cause the production of MTs with different protofilament numbers. These lead to the assembly of helical MT bundles with distinct chiralities within the cell. The helical MT arrays dictate specific patterns of cellulose deposition and cell elongation that produce helical twisting in the growing plant, with left-handed MT arrays giving rise to right-handed growth mutants and vice versa [19,20].

In 13 protofilament MT, each protofilament is offset from its neighbour to produce an apparent 3 start left-handed helix [21,22]. Around the helix, adjacent protofilaments are associated via homotypic α–α or β–β contacts, except for a 'seam', where α–β contact occurs [23,24]. The presence of this seam breaks the helical continuity and in this way allows protofilaments to the left and right sides of the seam to be determined.

(i) Microtubule motors

The polarity of MT construction implies that proteins can interact with the lattice in highly specific ways. In particular, motor molecules that utilize ATP hydrolysis to translocate along the MT have evolved to move along the MT from (− end) to (+ end) (anterograde) and vice versa (retrograde). Further, the motor can be fixed in position (for example attached to a stable protein network at the cell membrane or to a second MT) and it will produce MT translocation, but because motor travel with respect to the protofilament has limited torque, the MT does not act in the same way as the actin filament, such that helical chirality is relatively incidental to MT-based motility. Instead, individual protofilament construction and adjacent protofilament displacement is very important. In the cytoplasm, the anterograde motor is mainly cytoplasmic dynein; the retrograde motor is a kinesin 1, although other kinesins can participate in movement in either direction. Both well studied cytoplasmic dynein and kinesin 1 motors are dimeric molecules that execute processive 8 nm steps along the MT. Kinesin normally walks along a single protofilament, while cytoplasmic dynein utilizes two adjacent protofilaments and meanders slightly. Considerable effort has been expended to determine the exact interactions of the MT lattice and the motors [25–27].

(ii) Microtubule hooks

When incubated with tubulin under appropriate polymerization conditions, individual MTs grow small partial sheets of attached protofilaments at their sides. These sheets or hooks exhibit curvature that is related to MT polarity [28]; that is, the curvature is anticlockwise when the MT is viewed base (− end) to tip (+ end), and clockwise when the MT is viewed tip to base. Many studies have shown that virtually 100% of hooks correctly identify MT polarity in cells, which has been particularly important in studies of neuronal MTs, and has been confirmed by several other techniques [29]. Although hooks can form on different protofilaments, on cellular MTs hook curvature with respect to polarity is never reversed. (In axons where MT polarity is uniform, reversed hooks are almost certainly small numbers of MTs with reversed polarity.) It is not known if this is related to the MT seam, but if the seam is aligned facing you and the MT is drawn with the base at the bottom, tip at top, the hook is generated right to left, never left to right. This is a critical chirality in 13 protofilament MTs, which has been preserved throughout eukaryotic evolution and it may be related to the origin of the centriole. It may not be a feature of *in vitro* MTs of variable protofilament numbers.

(iii) The mitotic apparatus

One of the most important arrays of MTs in cells is the mitotic apparatus or spindle [30]. The spindle is set up so that pairs of chromatids will move to opposite poles by the end of anaphase and the cell can divide in two, a left and right daughter, which are sometimes, but not always, equivalent. The spindle is a transient structure with MT polymerization occurring around two separated organizing centres or poles. In animal cells, these organizing centres are centrosomes, each usually containing a pair of centrioles surrounded by pericentrosomal material, particularly γ tubulin that nucleates the 13 protofilament MTs whose (−) ends lie around the border of the centrosome. To produce the appropriate movements within the spindle the MTs interact with many different kinesins and with cytoplasmic dynein. Despite the complexity of MT interactions with the motors, the chromatids and poles, we can consider the left–right organization around the metaphase plate as equivalent to the actin organization around the Z line in muscle in that intrinsic MT polarity never changes, yet the MTs are organized with (+) ends in different directions so that new spatial properties, left and right sides of the spindle, left and right daughter cells, emerge.

The mitotic spindle can be set up so that division is asymmetric, which produces distinct left and right (or if oriented vertically anterior and posterior) daughter cells. Asymmetric divisions occur in mammalian tissues, in *Drosophila* and elsewhere. Development in *Caenorhabditis elegans*, where this process has been well studied, requires asymmetric division beginning at the one-cell stage [31,32]. Asymmetric divisions can set up different daughter cells, one of which remains a proliferative stem cell while the other differentiates. The mechanisms for setting up spindle asymmetry seem to have a common basis in different organisms; that is polarity proteins that help set up a cortical system of proteins whereby astral MTs are captured asymmetrical and spindles are oriented by dynein anchored to the cortical proteins [32,33].

(d) Basal bodies and centrioles

(i) Evolutionary considerations

While tubulins probably evolve in prokaryotes [34], the basal body or centriole is a distinctive eukaryotic organelle. It is a chiral organelle whose chirality determines distinctive features of both protistan structures and the vertebrate body plan. In early eukaryotes, represented by modern protists, there are only basal bodies. The spindle is a bundle of intranuclear MTs. True centrioles, which are basal bodies associated with spindle poles of a cytoplasmic spindle apparatus where the nuclear membrane has broken down, are not present. Presumably, capture of a basal body within a centrosome for control of spindle organization and templated centriolar reproduction in the centrosome with the cell cycle is a later evolutionary event.

In some protists (and in some plant and some mammalian cells), basal bodies seemingly arise en mass de novo from a cytoplasmic area resembling a viral factory. This led Satir *et al*. [35] to propose that the basal body arose from an encapsulated bacterial virus that invaded a protoeukaryotic cell cytoplasm at the beginning of eukaryotic evolution, where the viral genome subsequently was incorporated into the evolving eukaryotic nucleus, permitting centriolar latency [36]. This singular event would explain the unique chirality of the basal body. The alternative explanation, complex self-assembly [37], is less compelling [38]. Although features of the 13 protofilament MT discussed above might only permit this unique chirality, other protofilament arrangements and/or other tubulins might favour a reverse chirality, which is never seen.

Basal body MTs normally polymerize around a cartwheel assembled from SAS-6 protein dimers [39,40], leading to ninefold symmetry. The first MT to polymerize (subfibre A) is a complete 13 protofilament MT to which a partial second MT (subfibre B) is attached, much like a closed hook. Finally, a third partial MT (subfibre C) is attached to form a completed triplet at the base of the organelle. Looking base to tip, each triplet spirals outward from the cartwheel in a anticlockwise direction [41]. Looking base to tip, no organism has been found with clockwise spiralling triplet MTs, although this can be seen simply by looking tip to base (figure 1).

Although the standard mature basal body or centriole consists of a ring of nine triplet MTs at its base and nine doublet MTs, with subfibre B always in the same orientation to subfibre A, evolution has sometimes led to other doublet arrangements but with invariant chirality. A spectacular example is seen in the sperm of *Sciara* [43], where the centriole is a ring of 70 doublets.

(ii) Cilia

Basal bodies and centrioles grow cilia maintaining the same chirality of the doublet MTs. The MTs retain their polarity such that the ciliary tip contains the (+) ends of the doublets. Hooks can be grown on the ciliary MTs and these retain their anticlockwise curvature when viewed base to tip [44]. Not all basal bodies or centrioles grow cilia, but perhaps many which do not could be induced to undergo ciliogenesis under the right conditions. One protein which has been found to cap the centriole and prevent ciliogenesis is CP110; ciliogenesis is initiated when CP110 is removed and replaced by TTBK2 [45,46]. In many mammalian cells, for example embryo fibroblasts, there are pairs of centrioles in each G1 cell after mitotic division. If the cell enters division arrest (G_0), the older mother centriole grows a primary cilium, which is resorbed if the cell re-enters the cell cycle [47]. Primary cilia have an axoneme of nine doublet MTs (9 + 0 pattern) and are generally non-motile involved in cell signalling.

The chirality of the cilium becomes highly significant when cilia become motile. Motility has an important evolutionary advantage in that relatively fast behavioural response becomes possible. The axoneme of motile cilia is more complicated than that of primary cilia, with the details of structure now known at cryoelectron microscope resolution [48]. The two most obvious structural differences between non-motile and motile cilia are dynein arms, which run clockwise from subfibre A when viewed base to tip, and usually a central pair of single MTs, giving rise to the well-known 9 + 2 pattern. A line connecting the centres of the central singlet MTs is perpendicular to the axis that bisects the axoneme and a doublet (labelled no.1), passing between two doublet MTs labelled nos. 5 and 6 (figure 1). Because the arms always run clockwise, the arms on subfibre A of doublet no. 1 project toward and interact with subfibre B of doublet no.2. As dynein is a (−) end motor, when doublet 1 dynein is active it will slide doublet 2 tipward and the axoneme will begin to bend. Although the pattern and timing of doublet activity can vary, producing different beat phenotypes, one of the most common phenotypes involves activity of doublets 1–4 (the left side of the cilium, looking base to tip) to produce an effective stroke while doublets 6,7,8,9 respond passively, followed by a recovery stroke where dyneins on doublets 6–9 are active and 1–4 passive (figure 1). Stroke asymmetry may be presaged by a structure in the basal body that defines doublets 7,8,9,1,2 [49]. This model of ciliary motility is the switch point hypothesis [50].

In multiciliated cells, arrays of aligned basal bodies can be found. Sometimes the basal bodies are touching or almost touching, sometimes they are regularly spaced. When they grow cilia, the axes of the cilia are all parallel so that the effective strokes are all in the same direction, normally toward doublets 5–6, and the ciliary beat becomes coupled hydrodynamically.

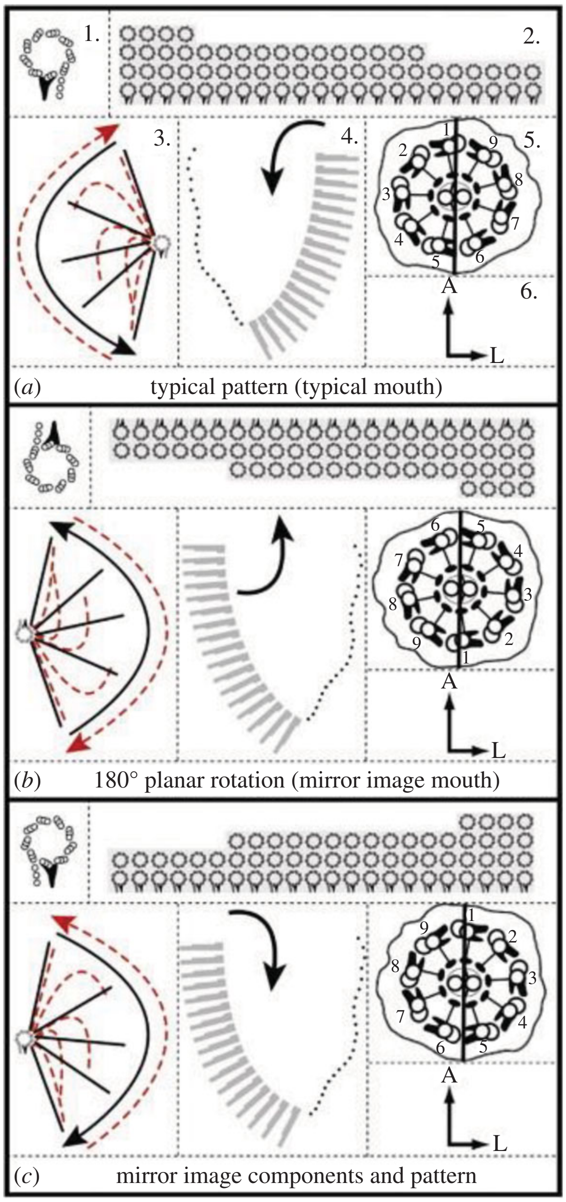

Figure 1. Diagrams of *Tetmemena* oral apparatus showing basal body arrangement and ciliary numbering (*a*) wt left side of mirror image cell (*b*) mirror image right side, actual arrangement due to 180° rotation with no change of basal body chirality (*c*) hypothetical true mirror image of wt using reversed basal body chirality. (1) The basal body. Seen from outside the cell looking inward (tip to base). In (*a*) and (*b*), the basal body is drawn as observed with its true universal chirality. Looking tip to base, subfibres B and C of the triplet MT lie clockwise to subfibre A, the complete 13 protofilament MT. Attached to the basal body is the dense triangular basal foot that identifies the direction of the effective stroke of the cilia that grow on these basal bodies. This is reversed by the 180° in (*b*). In (*c*), the true mirror image requires a reversed basal body chirality where looking tip to base, subfibres B and C run anticlockwise from subfibre A, which is never observed in any cell. (2) The arrangement of the rows of basal bodies in the oral apparatus. The rotation in (*b*) requires a different order of morphogenesis. (3) The ciliary stroke. Solid lines indicate the effective stroke with direction of beat shown. Dashed lines indicate the recovery stroke. The 180° rotation reverses the direction of the effective stroke. (4) The direction of the current created by the cilia (black arrow). The current brings food into the wt oral apparatus and the cytostome. (5) The 9 + 2 ciliary cross-section with the doublets numbered. The chirality of the basal body is maintained. Looking tip to base, dynein arms occupy the free side of suberfibre A and run anticlockwise toward the adjacent subfibre B. The effective stroke is in the direction of doublets 5–6. (6) Positional coordinates of the oral apparatus with respect to the cell: A, anterior; L, left. Reproduced from Bell *et al*., [42] with permission. Courtesy A. Bell and Develop. Biol. (Online version in colour.)

(iii) Consequences of basal body/ciliary chirality

The chirality of the basal body is related to the polarity (and chirality) of the cell as a whole. As an example, the ciliature of the ciliate protists is determined in part by the chirality of the basal body, as indicated by the rule of desmodexy [51]. Consider a line of basal bodies on a ciliate body. Looking from the outside of the cell inward along the row, kinetodesmal fibres extend apically from basal body to basal body. The basal bodies always lie to the right side of the fibres. Most mature basal bodies have a variety of satellite structures projecting from them. If they grow cilia, there are anchoring fibres that attach the basal body to the cell membrane and a basal foot that underlies doublets 5–6 and points in the direction of the effective stroke. An extensive discussion of protistan chirality is found elsewhere in this issue.

To extend this discussion, let us consider basal body chirality in connection with the production of mirror image doublets of certain ciliates [42]. Experimental manipulation of the spirotrich *Tetmemena* produced a mirror image doublet, which was capable of intraclonal propagation and regeneration after encystment. As seen in SEM, the cells have two distinct sets of ciliature, juxtaposed on their cortex with global mirror image symmetry, with a common anterior–posterior axis. Although the oral apparatus composed of rows of cilia starts out to assemble identically on both sides, because of the unique chirality of the basal bodies true mirror imaging of the oral apparatus is not possible. This is illustrated in figure 1, where in panel (*c*) true mirror imaging with the forbidden chirality of the basal body is shown.

As a consequence, the mirror image oral apparatus on the actual cell (shown in figure 1*b*) has the same organization as the wild-type oral apparatus (panel (*a*)), but is rotated by 180°. In this orientation, the enantiomophic form of the cilium is retained (looking tip to base, the dynein arms are counterclockwise from subfibre A of doublet n towards subfibre B of doublet $n + 1$) but anterior–posterior directions are reversed. As the activity of dynein on doublets 1–4 produces the effective stroke, the effective stroke of the cilia on the mirror image oral apparatus is reversed and ciliary beat actually pushes food away from the mouth! If the mirror image doublet is cut in two, the mirror image daughter eventually starves.

The positioning of basal bodies on the cell surface probably depends on the proteins that are involved in planar cell polarity. These have been identified in vertebrates in tissues with multiciliated cells including mammalian trachea [52]. As in the protistan oral apparatus, alignment of the basal bodies in the trachea so that they give rise to cilia, whose effective stroke is toward the pharynx, is critical. This depends on the unique chirality of the basal body and the ciliary axis. Mutations that cause misalignment give rise to a ciliopathy, primary ciliary dyskinesia (PCD), because the axes and effective strokes of the cilia become uncoordinated. In evolution, survival depends on global polarity information relayed to the cell in part by orientation of the MT and actin filament cytoskeletons and the chirality of the basal body to determine left and right coordinates within a defined anterior–posterior gradient.

Similarly, PCP proteins are involved in the positioning of the nodal cilia [53]. Because every basal body on the nodal cells is aligned in the same way with the axis of the node, the activation pattern of successive doublets in the nodal ciliary axonemes is equivalent and a fluid flow is created only in one direction from right to left sides of the node [54]. Like the basal bodies of spirotrichs, nodal basal bodies know left from right and this becomes reflected in gene activation patterns and then in organ morphogenesis in the vertebrate body. However, left–right determination in different organisms is not dependent on cilia, but rather is related to chiralities of MT and actin discussed earlier, and even in vertebrates the nodal flow hypothesis is probably not the whole story [55,56].

3. Conclusion

Supramolecular chirality emerges in self-assembly, where assembly produces polar filaments without an opposite enantiomer. This is seen in two main cytoskeletal elements of the eukaryotic cell, actin microfilaments and MTs.

The helical nature of polar actin microfilaments is used in building cell projections such as microvilli and also provides a screw direction to actin-based motility, with or without myosin motors.

In MTs, polar protofilament construction is determinative. Motor travel with respect to the protofilament has limited torque, such that helical chirality is relatively incidental to MT-based motility. In 13 protofilament MTs, the common MT *in vivo*, a seam is present that breaks helical continuity and defines left and right protofilaments. Hook or subfibre B growth on the MT is chiral.

Basal bodies are eukaryotic organelles that may derive from an encapsulated prokaryotic virus invasion of the proto-eukaryotic cytoplasm. They are arrays of short polar MTs usually polymerized around a cartwheel with ninefold symmetry with a unique chirality. Nowhere is the reverse chirality observed. Basal bodies evolve into mitotic centrioles. They usually grow cilia. The preserved basal body chirality is important in defining the direction of the effective stroke in motile cilia.

The alignment of these elements in the cell cytoplasm gives rise to emergent properties, including cellular tensegity [57] and the potential for cell differentiation and specialization, often by interaction with polarity proteins, which may be part of cell membrane scaffolds.

Competing interests. I declare I have no competing interests.
Funding. No funding has been received for this article.

References

1. Macnab RM. 1999 The bacterial flagellum: reversible rotary propellor and type III export apparatus. *J. Bacteriol.* **181**, 7149–7153.
2. Samatey FA, Imada K, Nagashima S, Vonderviszt F, Kumasaka T, Yamamoto M, Namba K. 2001 Structure of the bacterial flagellar protofilament and implications for a switch for supercoiling. *Nature* **410**, 331–337. (doi:10.1038/35066504)
3. Nishizaka T, Yagi T, Tanaka Y, Ishiwata S. 1993 Right-handed rotation of an actin filament in an *in vitro* motile system. *Nature* **361**, 269–271. (doi:10.1038/361269a0)
4. Yanagida T. 2007 Muscle contraction mechanism based on actin filament rotation. *Adv. Exp. Med. Biol.* **592**, 359–367. (doi:10.1007/978-4-431-38453-3_30)

5. Noji H, Yasuda R, Yoshida M, Kinosita Jr K. 1997 Direct observation of the rotation of F1-ATPase. *Nature* **386**, 299–302. (doi:10.1038/386299a0)
6. Tilney LG. 1975 Actin filaments in the acrosomal reaction of Limulus sperm. Motion generated by alterations in the packing of the filaments. *J. Cell Biol.* **64**, 289–310. (doi:10.1083/jcb.64.2.289)
7. Schmid MF, Sherman MB, Matsudaira P, Chiu W. 2004 Structure of the acrosomal bundle. *Nature* **431**, 104–107. (doi:10.1038/nature02881)
8. Tilney LG, Portnoy DA. 1989 Actin filaments and the growth, movement, and spread of the intracellular bacterial parasite, *Listeria monocytogenes*. *J. Cell Biol.* **109**, 1597–1608. (doi:10.1083/jcb.109.4.1597)
9. Mogilner A, Oster G. 1996 Cell motility driven by actin polymerization. *Biophys. J.* **71**, 3030–3045. (doi:10.1016/S0006-3495(96)79496-1)
10. Gerbal F, Chaikin P, Rabin Y, Prost J. 2000 An elastic analysis of *Listeria monocytogenes* propulsion. *Biophys. J.* **79**, 2259–2275. (doi:10.1016/S0006-3495(00)76473-3)
11. Cameron LA, Robbins JR, Footer MJ, Theriot JA. 2004 Biophysical parameters influence actin-based movement, trajectory, and initiation in a cell-free system. *Mol. Biol. Cell* **15**, 2312–2323. (doi:10.1091/mbc.E03-12-0913)
12. Tyska MJ, Mackey AT, Huang JD, Copeland NG, Jenkins NA, Mooseker MS. 2005 Myosin-1a is critical for normal brush border structure and composition. *Mol. Biol. Cell* **16**, 2443–2457. (doi:10.1091/mbc.E04-12-1116)
13. McConnell RE, Tyska MJ. 2007 Myosin-1a powers the sliding of apical membrane along microvillar actin bundles. *J. Cell Biol.* **177**, 671–681. (doi:10.1083/jcb.200701144)
14. Purves D, Augustine G, Fitzpatrick D, Katz L, LaMantia A, McNamara J, SM W. 2001 Hair cells and the mechansoelectrical transduction of sound waves. In *Neuroscience*, 2nd edn. Sunderland, MA: Sinauer Associates.
15. Huxley HE. 1969 The mechanism of muscular contraction. *Science* **164**, 1356–1365. (doi:10.1126/science.164.3886.1356)
16. Huxley AF, Peachey LD. 1961 The maximum length for contraction in vertebrate straiated muscle. *J. Physiol.* **156**, 150–165. (doi:10.1113/jphysiol.1961.sp006665)
17. Telley IA, Denoth J, Stussi E, Pfitzer G, Stehle R. 2006 Half-sarcomere dynamics in myofibrils during activation and relaxation studied by tracking fluorescent markers. *Biophys. J.* **90**, 514–530. (doi:10.1529/biophysj.105.070334)
18. Wade RH, Chrétien D, Job D. 1990 Characterization of microtubule protofilament numbers. How does the surface lattice accommodate? *J. Mol. Biol.* **212**, 775–786. (doi:10.1016/0022-2836(90)90236-F)
19. Ishida T, Thitamadee S, Hashimoto T. 2007 Twisted growth and organization of cortical microtubules. *J. Plant Res*. **120**, 61–70. (doi:10.1007/s10265-006-0039-y)
20. Hashimoto T. 2013 Dissecting the cellular functions of plant microtubules using mutant tubulins. *Cytoskeleton* **70**, 191–200. (doi:10.1002/cm.21099)
21. Amos L, Klug A. 1974 Arrangement of subunits in flagellar microtubules. *J. Cell Sci.* **14**, 523–549.
22. Chrétien D, Kenney JM, Fuller SD, Wade RH. 1996 Determination of microtubule polarity by cryo-electron microscopy. *Structure* **4**, 1031–1040. (doi:10.1016/S0969-2126(96)00110-4)
23. Mandelkow EM, Schultheiss R, Rapp R, Müller M, Mandelkow E. 1986 On the surface lattice of microtubules: helix starts, protofilament number, seam, and handedness. *J. Cell Biol.* **102**, 1067–1073. (doi:10.1083/jcb.102.3.1067)
24. Zhang R, Nogales E. 2015 A new protocol to accurately determine microtubule lattice seam location. *J. Struct. Biol.* **192**, 245–254. (doi:10.1016/j.jsb.2015.09.015)
25. Gigant B, Wang W, Dreier B, Jiang Q, Pecqueur L, Pluckthun A, Wang C, Knossow M. 2013 Structure of a kinesin-tubulin complex and implications for kinesin motility. *Nat. Struct. Mol. Biol.* **20**, 1001–1007. (doi:10.1038/nsmb.2624)
26. Imai H, Shima T, Sutoh K, Walker ML, Knight PJ, Kon T, Burgess SA. 2015 Direct observation shows superposition and large scale flexibility within cytoplasmic dynein motors moving along microtubules. *Nat. Commun.* **6**, 8179. (doi:10.1038/ncomms9179)
27. Redwine WB, Hernandez-Lopez R, Zou S, Huang J, Reck-Peterson SL, Leschziner AE. 2012 Structural basis for microtubule binding and release by dynein. *Science* **337**, 1532–1536. (doi:10.1126/science.1224151)
28. Heidemann SR, McIntosh JR. 1980 Visualization of the structural polarity of microtubules. *Nature* **286**, 517–519. (doi:10.1038/286517a0)
29. Baas PW, Lin S. 2011 Hooks and comets: The story of microtubule polarity orientation in the neuron. *Dev. Neurobiol.* **71**, 403–418. (doi:10.1002/dneu.20818)
30. Walczak CE, Heald R. 2008 Mechanisms of mitotic spindle assembly and function. *Int. Rev. Cytol.* **265**, 111–158. (doi:10.1016/S0074-7696(07)65003-7)
31. Cowan CR, Hyman AA. 2004 Asymmetric cell division in *C. elegans*: cortical polarity and spindle positioning. *Annu. Rev. Cell Dev. Biol.* **20**, 427–453. (doi:10.1146/annurev.cellbio.19.111301.113823)
32. Noatynska A, Gotta M. 2012 Cell polarity and asymmetric cell division: the *C. elegans* early embryo. *Essays Biochem.* **53**, 1–14. (doi:10.1042/bse0530001)
33. Stevermann L, Liakopoulos D. 2012 Molecular mechanisms in spindle positioning: structures and new concepts. *Curr. Opin Cell Biol.* **24**, 816–824. (doi:10.1016/j.ceb.2012.10.005)
34. Pilhofer M, Ladinsky MS, McDowall AW, Petroni G, Jensen GJ. 2011 Microtubules in *bacteria*: Ancient tubulins build a five-protofilament homolog of the eukaryotic cytoskeleton. *PLoS Biol.* **9**, e1001213. (doi:10.1371/journal.pbio.1001213)
35. Satir P, Guerra C, Bell AJ. 2007 Evolution and persistence of the cilium. *Cell Motil. Cytoskeleton* **64**, 906–913. (doi:10.1002/cm.20238)
36. Alliegro MC, Satir P. 2009 Origin of the cilium: novel approaches to examine a centriolar evolution hypothesis. *Methods Cell Biol.* **94**, 53–64. (doi:10.1016/S0091-679X(08)94002-4)
37. Jékely G, Arendt D. 2006 Evolution of intraflagellar transport from coated vesicles and autogenous origin of the eukaryotic cilium. *Bioessays* **28**, 191–198. (doi:10.1002/bies.20369)
38. Satir P, Mitchell DR, Jekely G. 2008 How did the cilium evolve? *Curr. Top. Dev. Biol.* **85**, 63–82. (doi:10.1016/S0070-2153(08)00803-X)
39. Kitagawa D *et al.* 2011 Structural basis of the 9-fold symmetry of centrioles. *Cell* **144**, 364–375. (doi:10.1016/j.cell.2011.01.008)
40. van Breugel M *et al.* 2011 Structures of SAS-6 suggest its organization in centrioles. *Science* **331**, 1196–1199. (doi:10.1126/science.1199325)
41. Gönczy P. 2012 Towards a molecular architecture of centriole assembly. *Nat. Rev. Mol. Cell Biol.* **13**, 425–435. (doi:10.1038/nrm3373)
42. Bell AJ, Satir P, Grimes GW. 2008 Mirror-imaged doublets of *Tetmemena pustulata:* implications for the development of left-right asymmetry. *Dev. Biol.* **314**, 150–160. (doi:10.1016/j.ydbio.2007.11.020)
43. Phillips DM. 1966 Observations on spermiogenesis in the fungus gnat *Sciara coprophila*. *J. Cell Biol.* **30**, 477–497. (doi:10.1083/jcb.30.3.477)
44. Euteneuer U, McIntosh JR. 1981 Polarity of some motility-related microtubules. *Proc. Natl Acad. Sci. USA* **78**, 372–376. (doi:10.1073/pnas.78.1.372)
45. Goetz SC, Liem Jr KF, Anderson KV. 2012 The spinocerebellar ataxia-associated gene *Tau tubulin kinase 2* controls the initiation of ciliogenesis. *Cell* **151**, 847–858. (doi:10.1016/j.cell.2012.10.010)
46. Xu Q, Zhang Y, Wei Q, Huang Y, Hu J, Ling K. 2016 Phosphatidylinositol phosphate kinase PIPKIgamma and phosphatase INPP5E coordinate initiation of ciliogenesis. *Nat. Commun.* **7**, 10777. (doi:10.1038/ncomms10777)
47. Satir P, Pedersen LB, Christensen ST. 2010 The primary cilium at a glance. *J. Cell Sci.* **123**, 499–503. (doi:10.1242/jcs.050377)
48. Nicastro D, Fu X, Heuser T, Tso A, Porter ME, Linck RW. 2011 Cryo-electron tomography reveals conserved features of doublet microtubules in flagella. *Proc. Natl Acad Sci. USA* **108**, E845–E853. (doi:10.1073/pnas.1106178108)
49. Geimer S, Melkonian M. 2004 The ultrastructure of the *Chlamydomonas reinhardtii* basal apparatus: identification of an early marker of radial asymmetry inherent in the basal body. *J. Cell Sci.* **117**, 2663–2674. (doi:10.1242/jcs.01120)
50. Satir BH, Wyroba E, Liu L, Lethan M, Satir P, Christensen ST. 2015 Evolutionary implications of localization of the signaling scaffold protein Parafusin to both cilia and the nucleus. *Cell Biol. Int.* **39**, 136–145. (doi:10.1002/cbin.10337)
51. Chatton E, Lwoff A. 1935 La constitution primitive de la strie ciliars des infusoires. La desmodexie. *Compt. Rend. Soc. Biol.* **118**, 1086–1172.
52. Vladar EK, Bayly RD, Sangoram AM, Scott MP, Axelrod JD. 2012 Microtubules enable the planar cell polarity of airway cilia. *Curr. Biol.* **22**, 2203–2212. (doi:10.1016/j.cub.2012.09.046)

53. Antic D, Stubbs JL, Suyama K, Kintner C, Scott MP, Axelrod JD. 2010 Planar cell polarity enables posterior localization of nodal cilia and left-right axis determination during mouse and *Xenopus* embryogenesis. *PLoS ONE* **5**, e8999. (doi:10.1371/journal.pone.0008999)

54. Hirokawa N, Tanaka Y, Okada Y, Takeda S. 2006 Nodal flow and the generation of left-right asymmetry. *Cell* **125**, 33–45. (doi:10.1016/j.cell.2006.03.002)

55. Coutelis J-B, González-Morales N, Géminard C, Noselli S. 2014 Diversity and convergence in the mechanisms establishing L/R asymmetry in metazoa. *EMBO Rep.* **15**, 926–937. (doi:10.15252/embr.201438972)

56. Davison A *et al.* 2016 Formin is associated with left-right asymmetry in the pond snail and the frog. *Curr. Biol.* **26**, 654–660. (doi:10.1016/j.cub.2015.12.071)

57. Ingber DE. 1993 Cellular tensegrity: defining new rules of biological design that govern the cytoskeleton. *J. Cell Sci.* **104**, 613–627.